

THEORETICAL DESIGN OF TITANIUM ALLOYS

M. MORINAGA, N. YUKAWA, T. MAYA, K. SONE and H. ADACHI*

Toyohashi University of Technology, Toyohashi, Aichi 440, Japan

*Hyogo University of Teacher Education, Yashiro-cho, Kato-gun, Hyogo 673-14, Japan

Abstract

A new method to the design of titanium alloys has been developed on the basis of the molecular orbital calculation of electronic structures. The two alloying parameters were determined theoretically for a variety of elements in bcc Ti and hcp Ti. The one is the bond order (called Bo) which shows the strength of the covalent bonding between Ti and an alloying element. The another is the metal d-orbital energy level (called Md) which correlates with the electronegativity and metallic radius of elements. The alloying behaviors are well understood using these parameters. For example, any titanium alloys can be classified into either the α , or $\alpha + \beta$, or β type by the aid of these parameters. The β transus temperatures can be estimated simply from alloy compositions. In addition, for β -type alloys the boundary between the slip and twin deformation can be located in the Bo - Md diagram. Utilizing these results the theoretical design of the heat-resisting α -type alloys and strong β -type alloys was performed successfully.

1. Introduction

Recently, a variety of new titanium alloys have been developed over the world. However, in most cases methods for the development are largely dependent on the trial-and-error experiments and some empirical rules. Therefore, the development is so inefficient and also expensive. In order to save cost and time necessary for alloy development, more fundamental approaches based on the solid theory are needed. In this paper, to meet with this need a theoretical method was developed and applied to the design of titanium alloys. A similar method had already been devised and employed successfully in developing Ni-based superalloys [1,2].

This method is based on the theoretical calculation of the electronic structures of titanium alloys by the discrete-variational (DV) $X\alpha$ cluster method [3]. New parameters which describe alloying behaviors were obtained for a variety of elements in titanium alloys.

2. DV- $X\alpha$ Cluster Calculations

In the DV- $X\alpha$ cluster method [4], an exchange correlation between electrons is included by means of a local exchange correlation potential, V_{xc} ,

$$V_{xc} = -3 \alpha \left[\frac{3}{8\pi} \rho(r) \right]^{1/3} . \quad (1)$$

Here, $\rho(r)$ is the electron density. The parameter α is fixed at 0.7, and the self-consistent charge approximation is used in the calculation.

A detailed explanation of the calculation is given elsewhere [5,6].

The electronic structures of bcc and hcp Ti containing alloying elements were calculated. In bcc Ti a titanium atom is surrounded by eight titanium atoms in the first-nearest-neighbor, and by six titanium atoms in the second-nearest-neighbor. Therefore, the cluster employed in the calculation is MTi_{14} , which is shown in Fig.1(a). In this cluster, a titanium atom in the central site is substituted for various alloying elements, M; Ti, V, Cr, Mn, Fe, Co, Ni, Cu (3d elements), Zr, Nb, Mo (4d elements), Hf, Ta, W (5d elements) and Al, Si, Sn (non-transition elements). The lattice parameter used is 0.3320 nm.

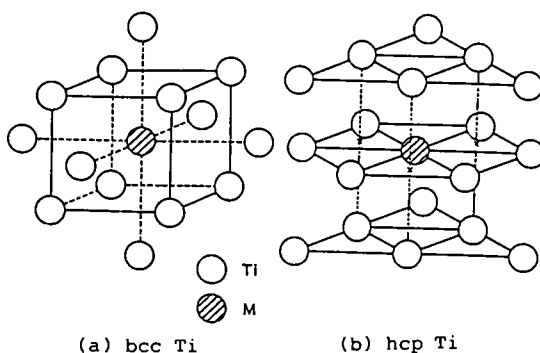


Fig.1 Cluster model used in the calculation

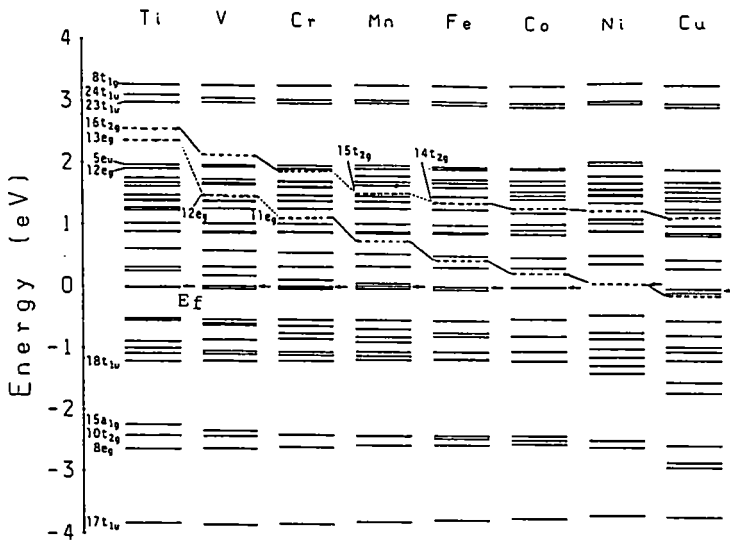


Fig.2 Energy level structure of bcc Ti containing 3d transition elements.

In hcp Ti, a titanium atom is surrounded by twelve titanium atoms in the first-nearest-neighbor, and by six titanium atoms in the second-nearest-neighbor. Therefore, the cluster used is MTi₁₈, as is shown in Fig.1(b). The lattice parameter is $a=0.2950$ nm and $c=0.4683$ nm. A series of calculations was carried out with varying elements, M, and two alloying parameters were determined theoretically for each element.

3. Electronic Structures and Alloying Parameters

3.1 Metal d-Orbital Level (Md)

The results of level structures are shown in Fig.2 for bcc Ti. In pure bcc Ti, the levels of $18t_{1u}$ to $5e_u$ are mainly originated from Ti 3d orbitals, namely, Ti 3d band where the Fermi level (E_F) lies. The lower energy levels of $17t_{1u}$ to $15a_1g$ and the upper energy levels of $13e_g$ to $8t_{1g}$ are the mixed states of Ti 3d, 4s and 4p. The calculated density of states resembles the result of band calculations.

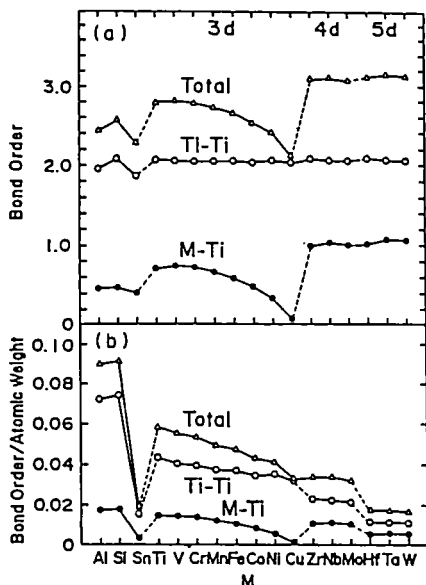


Fig.3 (a) Bond order and (b) ratio of bond order to atomic weight for M in bcc Ti.

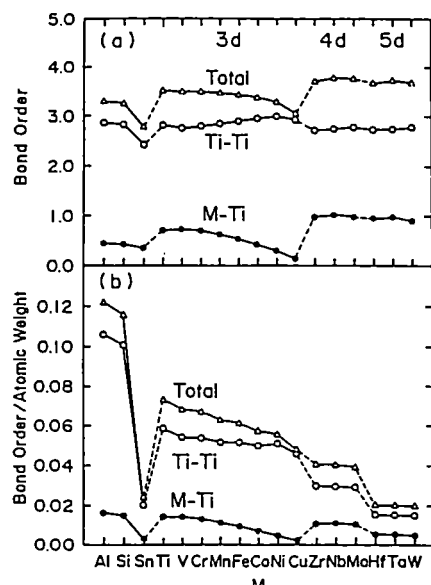


Fig.4 (a) Bond order and (b) ratio of bond order to atomic weight for M in hcp Ti.

In alloyed bcc Ti with 3d transition elements, energy levels due to the d orbitals of alloying elements, appear above the Fermi level. The e_g and t_{2g} levels, which are drawn by dotted lines in Fig.2, correspond to these levels. For the 4d⁹ and 5d² transition elements such levels appear and change systematically with the order of elements in the periodic table. The existence of these levels was also found in the calculation of alloyed Ni₃Al [5] and alloyed Fe [7]. It is noted that these metal-d levels correlate with the electronegativity and metallic radius of elements [5,7], both of which are classical parameters that have been applied to various metallurgical problems [8]. We defines M_d as the average of e_g and t_{2g} levels.

3.2. Bond Order (Bo)

The another important parameter is the bond order (Bo). This is a parameter to show the overlap populations of the electrons between atoms, and hence a measure of the strength of the covalent bonding between atoms. For transition metals and alloys, the d-d covalent bonds contribute largely to the cohesive energy. So, the bond order associated with the d-d electrons was calculated, and the results are shown in Fig.3(a) for bcc Ti and Fig.4(a) for hcp Ti. In the figure M-Ti and Ti-Ti are the bond orders between M-d and Ti-d and between Ti-d and Ti-d in a cluster, respectively and "total" means the sum of them. The M-Ti bond order depends largely on the alloying element M in either bcc or hcp Ti. It shows a small peak near V, and decreases continuously with the atomic number of M. Total bond order changes in a similar manner as the M-Ti bond order. The magnitude of the total bond order is higher in the 4d and 5d elements than in the 3d elements. There is a general resemblance in the bond order change with M between bcc Ti and hcp Ti.

According to our previous study [5,7], the elements with high bond order are principal alloying elements in the most alloys for structural applications. This is also true in the present case, since the main alloying elements in titanium alloys are V, Cr, Zr, Nb and Mo, all of which have high bond order. In order to allow for the density and the specific strength of alloys, the bond order of each element was divided by its atomic weight. The results are given in Fig.3(b) for bcc Ti and Fig.4(b) for hcp Ti. Fig.3(b) is very similar to Fig.4(b). The ratio of bond order to atomic weight is large for Al, (Ti), V. It may be said from this result that the selection of alloying elements in Ti-6Al-4V system is very resonable.

A good verification of the calculated bond orders may be seen in the atomic diffusion problem. The activation energy, Q , for the impurity diffusion in bcc Ti [9] correlates well with the bond order, as shown in Fig. 5. Q increases with Bo, since Q is probably proportional to the energy for cutting the bonds between M and Ti.

3.3. Definition of M_d and Bo for Alloy

For alloys, the average values of M_d and Bo are defined by taking the compositional average, and M_d and Bo are denoted as follows:

$$\overline{M_d} = \left[\sum_{i=1}^n x_i (M_d)_i \right] \quad (2)$$

$$\overline{Bo} = \left[\sum_{i=1}^n x_i (Bo)_i \right] \quad (3)$$

Table 1 List of Bo and M_d for Ti.

| | Bo | | M_d (eV) |
|-------|--------------|-------------|------------|
| | hcp alpha-Ti | bcc beta-Ti | |
| Ti | 3.513 | 2.790 | 2.447 |
| V | 3.482 | 2.805 | 1.872 |
| Cr | 3.485 | 2.779 | 1.478 |
| Mn | 3.462 | 2.723 | 1.194 |
| Fe | 3.428 | 2.651 | 0.969 |
| Co | 3.368 | 2.529 | 0.807 |
| Ni | 3.280 | 2.412 | 0.724 |
| Cu | 3.049 | 2.114 | 0.567 |
| Zr | 3.696 | 3.086 | 2.934 |
| 4d Nb | 3.767 | 3.099 | 2.424 |
| Mo | 3.759 | 3.063 | 1.961 |
| Hf | 3.664 | 3.110 | 2.975 |
| 5d Ta | 3.720 | 3.144 | 2.531 |
| W | 3.677 | 3.125 | 2.072 |
| Al | 3.297 | 2.426 | 2.200 |
| Si | 3.254 | 2.561 | 2.200 |
| Sn | 2.782 | 2.283 | 2.100 |

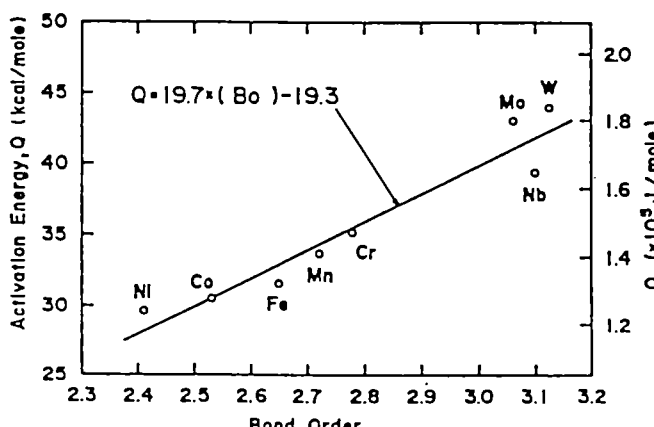


Fig.5 Correlation of the activation energy for the impurity-diffusion in bcc Ti with bond order.

Here, X_i is the atomic fraction of component i in the alloy, (M_{di}) and (B_{oi}) are the M_d and B_o values for component i , respectively. The values of (M_{di}) and (B_{oi}) are listed in Table 1. The summation extends over the components, $i=1,2,\dots,n$. Hereafter, unless otherwise mentioned, the (B_{oi}) and (M_{di}) values obtained for bcc Ti are employed for the analysis in this paper, since these parameters are relatively insensitive to the crystal structure.

4. Phase Stability of Titanium Alloys

4.1 Classification of Binary Phase Diagram

The three typical phase diagrams of Ti-M binary systems are shown in Fig.6 (A)-(C), where M is the transition element. (A) is the α and β perfect solid solution type, (B) is the β -isomorphous type and (C) is the β -eutectoid type. These three types can be distinguished clearly in the M_d vs B_o diagram, as shown in Fig.6. The phase diagram of the Ti-W system had been grouped into (C), but according to a recent study [10] it was revised and grouped into (B), in agreement with the present classification.

4.2 Estimation of β Transus

The β transus that is a phase boundary between the β and $\alpha+\beta$, was examined in various ternary alloy systems [11]. In Fig.7, the β transus of 973, 1073, 1173 and 1273K are drawn in the coordinates of B_o and M_d . The values of B_o and M_d were calculated from the alloy composition at the $\beta/\alpha + \beta$ phase boundary by using Eqs.(2) and (3). The constant β transus curves, for example, the four solid curves of a, b, d and i at 1273K are gathered together, independently of the alloy systems. As the β transus lowers from 1273K to 973K, the curves are shifted toward the higher B_o range. By approximating the group of curves at each temperature by a straight line, we may get the following relation among the B_o , M_d and the β transus (in absolute temperature, K);

$$\bar{B}_o = 0.326 \bar{M}_d - 1.950 \times 10^{-4} T + 2.217 \quad (4)$$

According to this equation, the β transus temperatures of several commercial alloys were estimated, and there was fairly good agreement between the measured and calculated temperatures.

4.3 Classification of Commercial Alloys into the α , $\alpha+\beta$ and β Types

Titanium alloys are commonly classified into the α , $\alpha+\beta$ and β types, according to the existing phases in alloys. In Fig.8 about forty commercial alloys are plotted in the B_o - M_d diagram by obtaining M_d and B_o values from their alloy compositions. It is apparent that the three types of alloys are clearly separated in this diagram. The No.6 alloy, Ti-8Mn, is located in the β field in spite of the $\alpha + \beta$ type alloy. However, this is not a contradiction, because Ti-8Mn is really an β -type alloy, but heat-treated in the $\alpha + \beta$ temperature range to improve the mechanical properties, and incidentally grouped into the $\alpha + \beta$ alloys. Utilizing this figure, we can predict the type of unknown alloy readily from the alloy composition, and no experiments are needed for this prediction.

In order to understand the alloying effect of each element in Ti, the B_o - M_d diagram was prepared for Ti-M binary alloys, and shown in Fig.9. When compared with Fig.8, we may see that

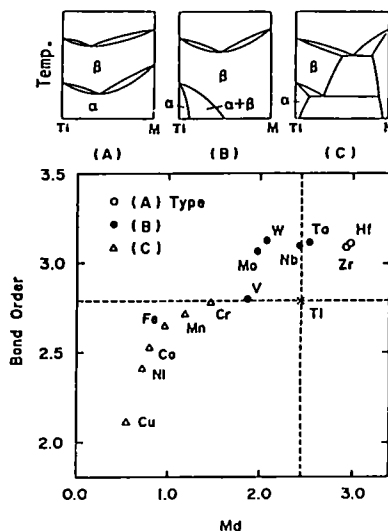


Fig.6 Phase diagrams of Ti-M binary alloys. Fig.7 Iso- β transus curves for various ternary alloys.

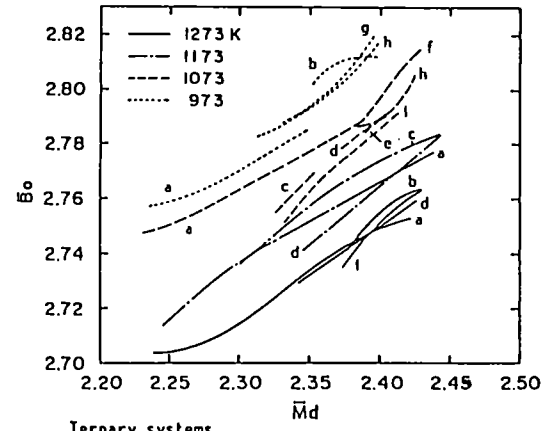


Fig.7 Iso- β transus curves for various ternary alloys.

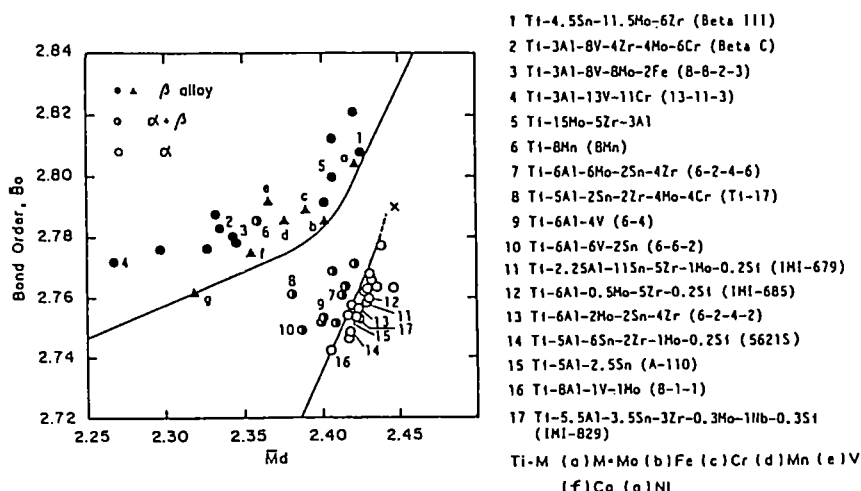


Fig.8 Classification of commercial alloys into the α , $\alpha + \beta$ and β types.

for instance, with increasing Al content the vector goes to the α phase field. This indicates that Al acts as an α -stabilizing element. In contrary, Mo and W are β -stabilizing elements since their vectors are directed toward the β phase field. These results agree with the well-known alloying behaviours of elements in Ti.

5. Alloy Design of α and β type alloys

5.1 α -type alloys

Heat-resisting α type alloys were designed so that the low temperature α phase could exist stably at higher temperatures. In other words, both the β transus (i.e. the $\beta/\alpha + \beta$ boundary temperature) and α transus (i.e. the $\alpha/\alpha + \beta$ boundary temperature) were tried to raise up as high as possible by changing alloy systems and compositions. This guide for the design was employed as creep properties were improved with increasing transus temperatures. Using Eq.(4) for β transus and an analogous equation obtained for the α transus, the alloys having maximum α and β transus were searched for under the condition that the α_2 (Ti-Al) phase does not occur in alloys.

It is interesting to note that IMI-829 and IMI-834 exhibit the highest calculated transus temperatures in the Ti-Al-Sn-Zr-Nb-Mo-Si system. This means that these are probably the best alloys in this system. Therefore, the other alloy systems were searched for. One candidate system is the Ti-Al-Sn-Zr-Ta-Mo-Si, which is the Ta substitution for Nb in the IMI alloys. According to our experiments on the tensile and creep properties at 823 K and on the oxidation resistance at 973 K, some designed alloys exhibited more balanced properties than the IMI alloys.

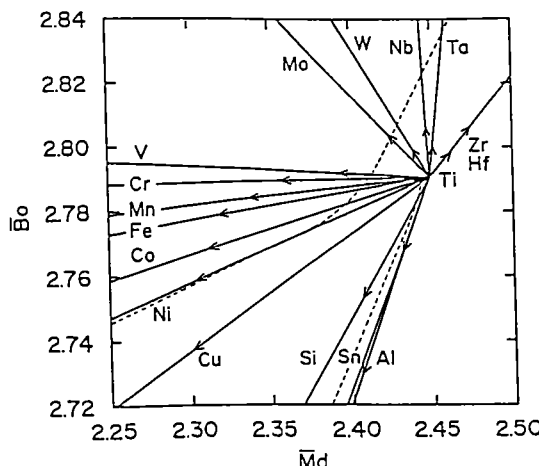


Fig.9 Phase stability change with alloying elements. The vector represents the location of Ti-10 mass.% M alloy.

5.2. β -type alloys

Several β -type alloys with high strength and good cold workability were designed with the aid of the $\text{Bo}-\text{Md}$ diagram. The β -type alloys are deformed by the either slip or twin mechanism, depending on the stability of the β phase. Namely, the slip mechanism works dominantly when the stability increases with the compositions of the β stabilizing elements in alloys. The boundary compositions between the slip and twin mechanism were determined by examining deformation bands which appear around a Vickers indentation. As shown in Fig.10, wavy slip bands appear when the slip mechanism is dominant, whereas straight twin bands appear when the twin mechanism is operating. For a variety of binary alloys such as Ti-V, Ti-Cr, Ti-Mn, Ti-Fe, Ti-Co, Ti-Nb, Ti-Mo, Ti-W and about fifty Ti-Al-V-Cr-Mo-Zr alloys with various compositions, this observation was carried out, and the results are summarized in the $\text{Bo}-\text{Md}$ diagram shown in Fig.10. It should be noticed that most practical alloys are located along this slip/twin boundary.

Using this $\text{Bo}-\text{Md}$ diagram, alloy design was performed, and several alloys (e.g. Ti-V-Cr-Fe-Al) located near 15-3 alloy in the diagram showed good ductility as well as high strength.

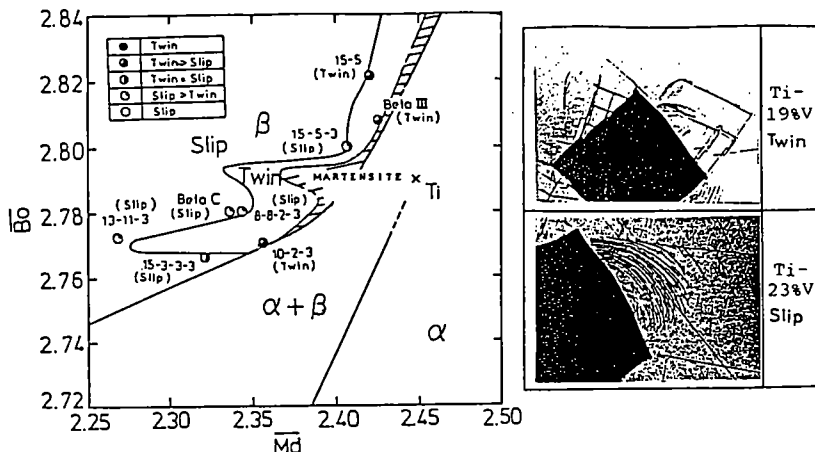


Fig.10 Slip/twin boundary and the martensite region shown in $\text{Bo}-\text{Md}$ diagram.

6. Conclusions

Based on the electronic theory, a new method was developed for the design of titanium alloys. The phase stability and the other alloy properties can be well predictable from this method. The usefulness of the method was proved through the practical design of heat-resisting α -type alloys and strong β -type alloys.

Acknowledgements

The authors acknowledge the staff of the Computer Center, Institute for Molecular Science, Okazaki National Research Institute, for the use of the HITAC M-680H and S-810 computers. This research was supported in part by the Toray Science Foundation.

References

- [1] M. Morinaga, N. Yukawa, H. Adachi and H. Ezaki, Superalloys 1984, eds. M. Gell et al., 1984 (Warrendale, Pennsylvania: The Metallurgical Society of AIME), pp.523-532.
- [2] N. Yukawa, M. Morinaga, H. Ezaki and Y. Murata, High Temperature Alloys for Gas Turbines and Other applications 1986, eds. W. Betz et al., 1986 (Dordrecht: D. Reidel Publishing Company), Part II, pp.935-944.
- [3] M. Morinaga, N. Yukawa and H. Adachi, Tetsu-to-Hagane, 72 (1986) 555.
- [4] J. C. Slater, Quantum Theory of Molecules and Solids, Vol.4 (New York: McGraw-Hill).
- [5] M. Morinaga, N. Yukawa and H. Adachi, J. Phys. Soc. Jpn., 53(2) (1984) 653.
- [6] M. Morinaga, N. Yukawa, H. Adachi and T. Mura, J. Phys. F: Met. Phys. 17 (1987) 2147.
- [7] M. Morinaga, N. Yukawa and H. Adachi, J. Phys. F: Met. Phys. 15 (1985) 1071.
- [8] W. Hume-Rothery and G. V. Raynor, Structure of Metals and Alloys, 1954 (London: Institute of Metals).
- [9] J. Askill, Tracer Diffusion Data for Metals, Alloys, and Simple Oxides (New York: McGraw-Hill).
- [10] W. G. Moffatt, The Handbook of Binary Phase Diagrams, Vol.2 (Schenectady, NY: General Electric Company).
- [11] E. K. Molchanova, Phase Diagrams of Titanium Alloys, 1965 (Jerusalem: Israel Program for a Scientific Translations).